Accepted Manuscript

Title: Influence of Lu content on $(Lu_xGd_{1-x})_2SiO_5$ oxyorthosilicates grown by Laser Floating Zone: structural studies and transparency

Authors: F. Rey-García, A.J.S. Fernandes, F.M. Costa

PII: S0025-5408(18)30714-1
DOI: https://doi.org/10.1016/j.materresbull.2018.04.058
Reference: MRB 9996

To appear in: *MRB*

Received date: 28-7-2017
Revised date: 8-3-2018
Accepted date: 30-4-2018

Please cite this article as: Rey-García F, Fernandes AJS, Costa FM, Influence of Lu content on $(Lu_xGd_{1-x})_2SiO_5$ oxyorthosilicates grown by Laser Floating Zone: structural studies and transparency, *Materials Research Bulletin* (2010), https://doi.org/10.1016/j.materresbull.2018.04.058

Influence of Lu content on $(Lu_xGd_{1-x})_2SiO_5$ oxyorthosilicates grown by Laser Floating Zone: structural studies and transparency

F. Rey-García*, A.J.S. Fernandes, F.M. Costa
Departamento de Física & I3N, Universidade de Aveiro, 3810-193 Aveiro, Portugal
*mail: frgarcia@ua.pt

GRAPHICAL ABSTRACT

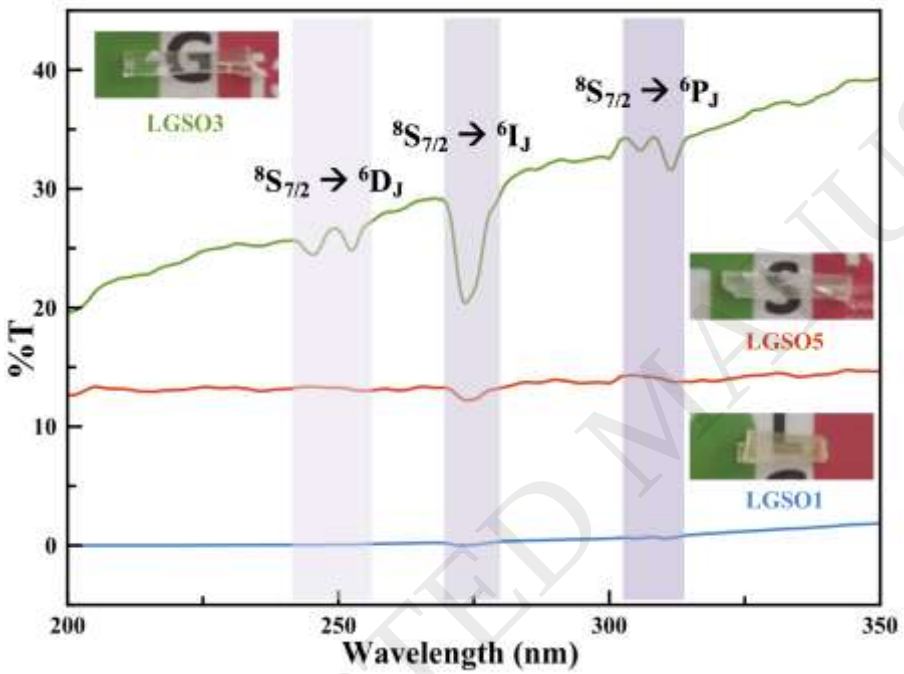

HIGHLIGHTS

- Lutetium gadolinium oxyorthosilicates (LGSO) produced by Laser Floating Zone (LFZ).
- High growth rate in air of LGSO ($(Lu_xGd_{1-x})_2SiO5$, x=0.1, 0.3 and 0.5) single crystal.

- Transparency and energy transfer band intensity tailored by the Lu/Gd amount.

ABSTRACT

Lutetium gadolinium oxyorthosilicates (LGSO, $(Lu_xGd_{1-x})_2SiO_5$, x=0.1, 0.3 and 0.5)) were obtained by the Laser Floating Zone (LFZ) in air at 10 mm/h, much faster than those produced by the standard Czochralski method. The LGSO fibres were structural and optically characterized. Scanning electron microscopy (SEM/EDS) allowed observing homogeneous monophasic crystalline fibres that obey the expected phase transition from $P2_1/c$ to C2/c monoclinic structures, as revealed by X-Ray diffraction and Raman spectroscopy. Finally, transmission studies in the near UV to visible range allowed to quantify the transmission and to appraise the presence of energy transfer bands that favor their use as host materials in photonic applications.

Keywords: LGSO, Oxyorthosilicates, Crystal growth, Phase transition, Laser Floating Zone

INTRODUCTION

Gadolinium (GSO) and lutetium (LSO) oxyorthosilicates have been studied in different photonics **applications [1-4]**, however the interest of researchers has progressively been directed towards mixed oxyorthosilicates of lutetium and gadolinium (LGSO) [5-8] due to three important reasons [9-11].

Lutetium, as pure Lu_2O_3 precursor, is an expensive material that significantly increases production costs when it is employed on photonic materials production. Thus, co-doping with gadolinium ions from, for example, cheaper Gd_2O_3, allows reducing production associated costs without affecting the structural and optical properties. On the other hand, gadolinium oxyorthosilicate single crystals **tend** to develop cracks during growth. In this case, lutetium doping has been employed **aiming to** reduce thermal stress and, therefore, avoid crack formation. Finally, compared to pure LSO materials, the gadolinium doping significantly reduces the melting point.

Since Loutts et al. [12] produced LGSO for first time in 1997, to our knowledge, most studies related to its synthesis involve the use of the Czochralski (CZ) method [5-12]. Only Zorenko et al. [13, 14] reported other technique such as liquid phase epitaxy for the growth of single crystalline films. **To our knowledge, De la Fuente et al. [15] produced for first time Nd-doped fibres of LSO and GSO in Ar+O_2 atmosphere by the alternative Laser Floating Zone (LFZ) technique.** Recently, **pure** GSO [**16**] and LSO [**17**] have been obtained for first time in air at high pulling rates employing **this technique [16-17]**. However, the growth behavior of these oxyorthosilicates under the LFZ processing is quite different [**18**]. Thus, while single crystalline monoclinic fibres of Gd_2SiO_5 can be obtained in air at 10 mm/h [**16**] as expected from crystal growth theory [**19**], eutectic fibres of LSO/Lu_2O_3 are obtained for the Lu_2O_3:SiO_2 system **at the same pulling rate** [**17**]. **This contradictory behavior relates to the high difference between precursors melting points [17, 18], specifically considering each oxide type structure [20]. Gadolinium oxide starts a structural transition from cubic ($Ia\bar{3}$) C-type to monoclinic (C2/m) B-type at 1500 ºC. However, lutetium oxide only presents the cubic ($Ia\bar{3}$) C-type structure, remaining thermally stable until 2400 ºC [21], well above the silicon oxide boiling point (2230 ºC). Thus, silicon oxide can be evaporated before reacting with molten lutetium oxide.** This fact, together with the interest **of improving the** structural and optical properties of GSO fibres produced by LFZ **and the possibility to avoid that effect**, justifies a study **on** gadolinium lutetium oxyorthosilicates developed **by** this technique.

Thus, the aim of this work was the study of the Lu doping influence on the structural and physical properties of LGSO materials processed by the LFZ technique. Compositions of $(Lu_xGd_{1-x})_2SiO_5$ (LGSO) oxyorthosilicate, with x= 0.1, 0.3 and 0.5, were studied. The morphology and structural characteristics of the LGSO fibres produced were assessed by scanning electron microscopy

(SEM/EDS), Raman spectroscopy and X-ray diffraction (XRD) analysis. Finally, transmission studies on UV-Vis range were carried out to confirm if optical properties associated to intra $4df^7$ transitions of Gd^{3+} ions related to energy transfer band that allows their use as laser host material are kept. The transparency was evaluated by absorption experiments in the **visible - near UV region**.

EXPERIMENTAL

Crystal growth

$(Lu_xGd_{1-x})_2SiO_5$ (LGSO) oxyorthosilicate fibres, with x = 0.1, 0.3 and 0.5, were grown by the LFZ technique [**16, 17, 22**]. Feed and seed rod precursors for LFZ growth were prepared by mixing Gd_2O_3 (Mateck, 99.999%), Lu_2O_3 (Shangai Co., 99.99%) and SiO_2 (Aldrich, 99,99%) in agate ball mill commercial powders at the stablished proportions (Table I). Polyvinyl alcohol (PVA) was added to bind the powder mixture (PVA 0.1 g/ml) that was further extruded into cylindrical rods with diameters around 1.5 mm.

The LFZ equipment comprises a 200 W CO_2 laser (Spectron, GSI group) coupled to a reflective optical setup producing a circular crown-shaped laser beam promoting a uniform radial heating [**18, 22**]. This way, fibres with diameters around 1.5 mm and 10-40 mm in length were grown in descendent direction at 10 mm/h pulling rate on air at atmospheric pressure under a rotation speed of 5 rpm **from rods previously densified at 100 mm/h** [**16, 17**]. **Given the densified nature of the feed rods, both feed and seed rates were the same, 10mm/h.** Table I summarizes **the studied compositions and corresponding** growth conditions. **Those of pure GSO and LSO (x = 0 and x = 1, respectively) previously grown by LFZ in the same conditions [16, 17], are also included for reference**.

Table I. **Composition and** LFZ experimental conditions, **compared to those of pure GSO [16] and LSO [17].**

Sample	Nominal formula	Diameter (mm)	Pulling rate (mm/h)	Power (W)	Ref.
GSO	Gd_2SiO_5	1.5	10	72	**16**
LGSO-1	$(Lu_{0.1}Gd_{0.9})_2SiO_5$	1.5	10	67	-
LGSO-3	$(Lu_{0.3}Gd_{0.7})_2SiO_5$	1.5	10	58	-
LGSO-5	$(Lu_{0.5}Gd_{0.5})_2SiO_5$	1.5	10	64	-
LSO	Lu_2SiO_5	2	10	92	**17**

Structural and Optical characterization

The fibres microstructure was characterized by scanning electron microscopy (SEM, TESCAN Vega 3SEM) fitted with energy dispersive X-ray spectroscopy (EDS) on polished surfaces of longitudinal and transversal fibre sections.

The structural characterization of the fibres was firstly accomplished by X-ray powder diffraction (XRD) experiments with a EMPYREAN X-ray diffractometer (PANalytical) using a Cu anode, while the data were fitted with the analytical software HighScore Plus. The fibres were smashed into powder to perform the standard Bragg-Brentano X-ray diffraction analysis. Room temperature (RT) µ-Raman spectroscopy using the 441.6 nm line of a He–Cd laser (Kimmon IK Series) was also performed to complete structural characterization. A Horiba Jobin-Yvon HR800 instrument fitted with a 100x magnification lens with 0.9 numerical aperture and a minimum spot size < 2 µm was employed to perform the Raman studies.

The transmission measurements were carried out in a Shimatzu UV-2100 spectrometer which was used in the range of 190-900 nm with deuterium and tungsten lamps as excitation sources. Fibres polished on plane-parallel configuration were employed as measuring samples.

RESULTS AND DISCUSSION

Lutetium-gadolinium oxyorthosilicate crystalline fibres have been successfully obtained by LFZ, as shown in Fig. 1, where plane parallel-polished fragments of materials developed are shown. When

observed at naked eye, samples differ on transparency, being both LGSO-1 and LGSO-5 fibres translucent. In its turn, the LGSO-3 sample is transparent, being clearly distinguishable the colors of the image background and displaying higher sharpness. Additionally, the LGSO-1 sample presents a yellowish tone **like** that observed in GSO samples [**16**]. In fact, its composition is the closest to the pure gadolinium oxyorthosilicate, for which the Lu content is minimum. On the other hand, the LGSO-5 seems to be neutral translucent allowing us to consider that the LSO behavior could be achieved at low pulling rates for Lu_2O_3-SiO_2 systems in lutetium oxyorthosilicates with high amounts of Gd in opposite to **not doped** systems processed by LFZ that produced ceramic biphasic samples [**17**]. Comparing to the **pure** GSO processed by LFZ [**16**], the LGSO-3 fibre exhibits a lower amount of internal cracks and fractures. This corroborates the bibliography, since LGSO possesses better plasticity and lower tendency to crack than **pure** GSO [5, 9-11]. The cracks observed in Fig. 1 are mainly originated from the cutting and polishing steps. These first results together with the advantages promoted by LFZ technique such as no seed needed or processing under ambient conditions should drastically reduce fabrication costs favoring its value over standard methods like CZ. Nevertheless, the structure and compositions must be studied in detail.

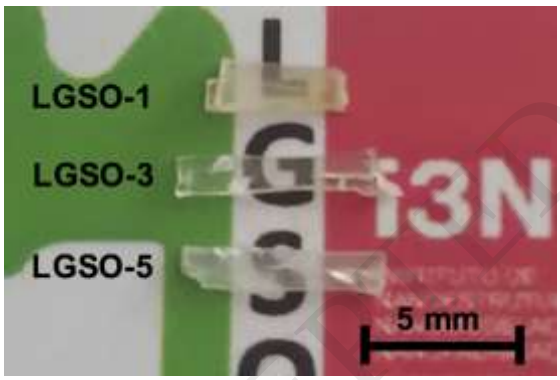

Fig. 1 Photograph of bulk plane parallel-polished fragments of LGSO-1 (top), LGSO-3 (middle) and LGSO-5 (bottom) samples grown at 10 mm/h.

SEM analysis of the fibres grown by LFZ reveals that the longitudinal sections of all LGSO samples (Fig. 2) are homogeneous along the entire surface with uniform contrast and without visible grain boundaries, suggesting **single crystal** [**16, 17**]. Moreover, no significant cracks due to **stresses** are

observed at the border of the fibres (Fig. 2b). However, small cracks and internal defects probably due to quick crystallization and/or polishing processes are observed inside the fibres. Considering that the LGSO-5 fibre presents the major **number** of defects and that all the fibres were polished together, it **could** be assumed that this sample corresponds to the weaker material. So, the introduction of the Lu could induce a reduction on the structural stability of the LGSO fibres grown by LFZ. Accordingly, Dominiak-Dzik et al. [9], observed how Lu^{3+} substitution by Gd^{3+} ions on $(Lu_{1-x}Gd_x)_2SiO_5$:Dy single crystals grown by CZ decreases melting point, reducing stress and, therefore, possible cracks on oxyorthosilicate structure. **However, observing the samples appearance (Fig. 1), seems to be a non-monotonic behavior with the Lu doping. Indeed, while LGSO-1 and LGSO-5 present similar transparency, the LGSO-3 sample is the best of the set. Thus, structure and composition were studied in detail to understand its influence on optical properties.**

Fig. 2 Longitudinal section SEM micrographs (500X) of (a) LGSO-1, (b) LGSO-3 and (c) LGSO-5 fibres.

On the other hand, EDS analysis performed confirms the homogeneity of fibres, revealing a uniform composition without presence of secondary or eutectic phases, as could be expected from the LFZ treatment of Lu_2O_3/SiO_2 mixtures [**17**]. It must be noted that compositions calculated from EDS analysis are close to initial mixtures (Table II), **in opposition** to compositional dissimilarity observed for LGSO materials developed by conventional CZ method [5-12]. Anyway, **aiming to** reduce fabrication costs associated to LSO materials by standard methods like CZ, **LFZ results more** suitable from the environmental point of view (growth in ambient conditions) and time reduction. Moreover, the introduction of dopants avoids the formation of eutectic phases as Rey-Garcia et al. [**17**] reported for the LFZ processing of the Lu_2O_3/SiO_2 system at 10 mm/h.

Table II. Initial and calculated compositions determined by EDS analysis.

Sample	Initial composition	EDS calculated composition
LGSO-1	$(Lu_{0.1}Gd_{0.9})_2SiO_5$	$(Lu_{0.12}Gd_{0.88})_2SiO_5$
LGSO-3	$(Lu_{0.3}Gd_{0.7})_2SiO_5$	$(Lu_{0.31}Gd_{0.69})_2SiO_5$
LGSO-5	$(Lu_{0.5}Gd_{0.5})_2SiO_5$	$(Lu_{0.53}Gd_{0.47})_2SiO_5$

XRD analysis of the LGSO powders puts in evidence the crystallinity degree and the monophasic nature of these samples together with the **expected** structural transition. The diffractograms recorded for LGSO sample were compared to those of un-doped GSO [**16**], LSO [**17**] and corresponding XRD ICDD cards [**23**], 04-009-2670 and 04-013-1146, respectively, to achieve a good understanding. As we can observe on Fig. 3, LGSO-1 presents the monoclinic $P2_1/c$ structure while the LGSO-3 and LGSO-5 have a monoclinic C2/c structure. These results follow the structural phase transition observed for $(Lu_xGd_{1-x})_2SiO_5$ (LGSO) oxyorthosilicate materials that exhibit a GSO-type ($P2_1/c$) structure for $x<0.15$ and LSO-type (C2/c) when $x>0.17$ [5-14].

The phase transition rule can be explained from the different atomic size together with the ion surrounding. Recently, Ryba-Romanowski et al. [6] related the crystal transition of LGSO doped compositions to the differences of nearest surrounding rare earth ions. Two types of Gd sites, Gd1 and Gd2, are present at the GSO lattice, presenting both different coordination number and local symmetries (CN=9, C_{3v} and CN=7, C_s, respectively). These promote the polyhedrons GdO_9 and GdO_7 depicted in Fig. 4. However, in the case of the lutetium oxyorthosilicate, both lutetium ions and, therefore, the LuO_6 (Lu1) and LuO_7 (Lu2) polyhedrons, present the C_s local symmetry [6]. The C_{3v} point group presents higher steric effect while C_s has only one plane of symmetry. This, together with the fact that monoclinic $P2_1/c$ unit cell is smaller than the C2/c **causes that the inclusion of Lu^{3+} ions strongly affects the crystal structure, despite their smaller ionic radius**. This way, the LGSO with GSO structure type allows low Lu doping. On the other hand, the steric effect is minor on a C2/c type structure and, furthermore, the Lu sites can be both occupied with larger size ions, such as Gd^{3+} or Ce^{3+} [6]. So, the symmetry degree of freedom should be quite higher than for GSO type. This implies that higher amounts of doping could be achieved. In fact, doping levels from x=0.17 up to 0.8 have been achieved for different researchers in the crystals with $(Lu_xGd_{1-x})_2SiO_5$ compositions [5-14, **24**].

For this reason, LGSO-3 and LGSO-5 have the C2/c crystal group although the Lu doping level is quite different.

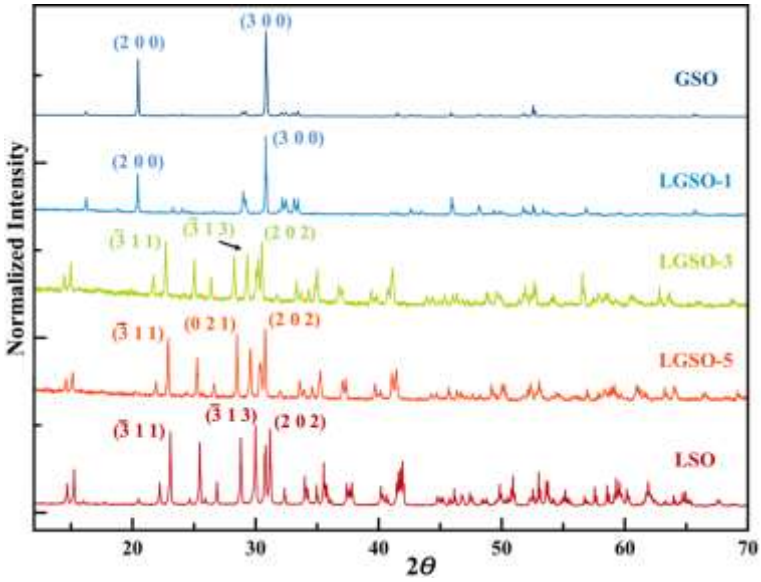

Fig. 3. Normalized XRD diffractograms of GSO (dark blue line, [**16**]), LGSO-1 (blue line), LGSO-3 (green line), LGSO-5 (orange line) and LSO (red line, [**17**]) sample powders. Most intense peaks are noticed.

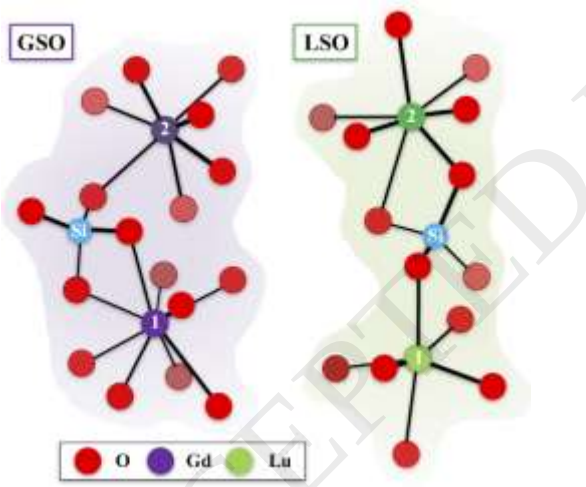

Fig. 4. **Structural** scheme of Gd_2SiO_5 (GSO, left) and Lu_2SiO_5 (LSO, right) **units** [5, 8, 9].

Coming back to LGSO fibres structure, LGSO-1 matched with the 01-080-9851 XRD card ICDD [**23**] that refers to the monoclinic $P2_1/c$ $(Lu_{0.15}Gd_{0.85})_2SiO_5$ single crystal produced by Glowacki et al. [10] through CZ method. It must be noted that, despite the exhaustive milling, the powders diffractogram

maintains some degree of preferential orientations promoting defined reflections of the crystallographic planes more intense than others as was observed by Rey-García et al. [**16**] for the GSO grown by LFZ. This fact let us to confirm the high crystallinity degree of the fibres produced. The most intense peaks, located at 20.4º and 30.8º, would correspond to (2 0 0) and (3 0 0) planes respectively, extrapolating from the 01-080-9851 XRD card that referred the monoclinic $(Lu_{0.15}Gd_{0.85})_2SiO_5$ oxyorthosilicate.

The diffractograms of LGSO-3 and LGSO-5 are isostructural with the 00-061-0488 and the 00-061-0369 XRD cards from the JCDD PDF4+ (Join Committee for Diffraction Data, 2016) bibliographic data [**23**], corresponding to single crystal oxyorthosilicates with $Lu_{0.36}Gd_{1.64}SiO_5$ and $Lu_{1.33}Gd_{0.67}SiO_5$ compositions, respectively. Although a multitude of peaks can be observed in Fig. 3, the most intense ones are placed around similar degree values in both LGSO and un-doped LSO when extrapolated from the equivalent XRD cards. The peaks placed at 30.5º and 30.8º correspond to (2 0 2) plane and are the most intense in LGSO samples, while for the LSO the most intense is placed at 29.9º corresponding to ($\bar{3}$ 1 3) plane [**17**]. Furthermore, the signals associated to ($\bar{3}$ 1 1) plane are included between the three most intense peaks of each phase (Table III). All considered, it can be concluded that the introduction of Gd^{3+} ions on Lu_2O_3-SiO_2 system avoids the formation of binary-eutectic fibres [**17**] **since the melting temperature is decreased, hampering the SiO_2 evaporation, unavoided for the Lu_2O_3 cubic ($Ia\bar{3}$) C-type structure high melting point [21]. Therefore**, the LSO C2/c monoclinic **structure remains inside** a Lu/Gd ratio ranging from 0.2 ($(Lu_xGd_{1-x})_2SiO_5$, x>0.17) to 1 (LGSO-5).

Table III. XRD most intense peaks, corresponding planes and intensity for LGSO-3, LGSO-5 and LSO [**17**].

LGSO-3			LGSO-5			LSO [**17**]		
Peak	Plane	Intensity (%)	Peak	Plane	Intensity (%)	Peak	Plane	Intensity
22.7º	($\bar{3}$ 1 1)	99.7	22.9º	($\bar{3}$ 1 1)	89.8	23.2º	($\bar{3}$ 1 1)	92.6
29.3º	($\bar{3}$ 1 3)	85.8	28.5º	(0 2 1)	93.7	29.9º	($\bar{3}$ 1 3)	100
30.5º	(2 0 2)	100	30.8º	(2 0 2)	100	31.2º	(2 0 2)	95.5

Fig. 5 shows the Raman spectra of the LGSO samples compared with reported GSO and LSO Raman spectra [**16, 17, 25**]. The spectra were normalized to the intense peak recorded around 890 cm^{-1} that defines the type of oxyorthosilicate present [**25**]. **Several** number of peaks have been recorded from each as-grown fibre. This fact is typical of oxyorthosilicates, **since** $24A_g+16B_g$ to $24A_g+18B_g$

vibration modes can be observed for GSO and LSO undoped materials, respectively [**25**]. The first approach allows observing how LGSO-1 spectrum is **close** to pure GSO [**16**] as expected. However, as Lu amount is increased, the Raman spectrum features change to shapes closer to un-doped LSO [**17**], as observed in LGSO-5 sample. On the other hand, the LGSO-3 fibre presents an intermediate spectrum.

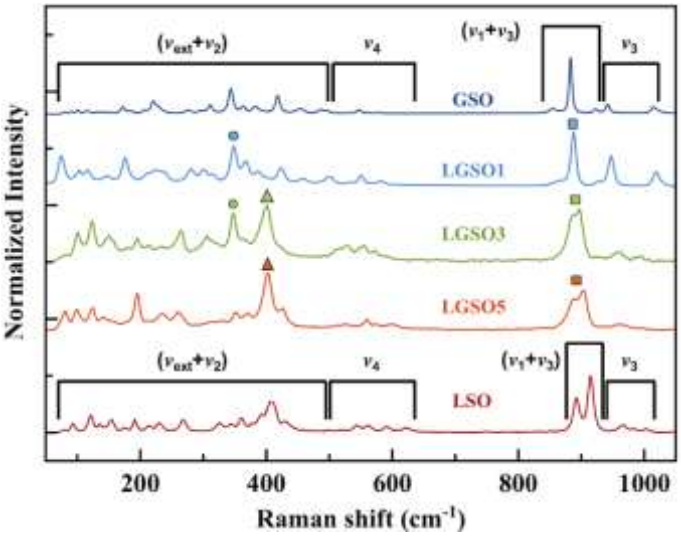

Fig. 5. Normalized Raman spectra of GSO (dark blue line, [**16**]), LGSO-1 (blue line), LGSO-3 (green line), LGSO-5 (orange line) and LSO (red line, [**17**]). GSO and LSO regions have been represented accordingly to Voron'ko et al. [**25**] notation. Bands discussed on Results section are denoted by circles, triangles and squares with the corresponding **color**.

By the way, the Raman spectra of the LGSO oxyorthosilicates developed by LFZ were studied according to the Voron'ko et al. notation [**25**]. Thus, the Raman spectrum of one defined oxyorthosilicate can be divided into four vibrational regions denoted by ν_3, $\nu_1+\nu_3$, ν_4 and $\nu_{ext}+\nu_2$. Thus, the (ν_1) - (ν_4) modes correspond to the free $[SiO_4]^{4-}$ internal vibrations in the reduced C_1 symmetry of the monoclinic lattice and the (ν_{ext}) mode to the external oscillations related with the translation of the $[MO_4]$-complexes [**25**]. It must be mentioned that in compounds with tetrahedral oxyanions, there is a characteristic energy gap between 600 and 800 cm^{-1} [10], which is also present here, and that usually separates internal bending and stretching vibrations of tetrahedral molecules. However, as Glowacki et al. [10] reported, the stretching vibrations of RE-O bonds can be recorded in the range of bending vibrations, hindering the clear identification of the peaks with their corresponding vibration modes.

Returning to the experimental results, the main feature takes place on the high frequency region ($\nu_1+\nu_3$). A-type oxyorthosilicates present at around 900 cm^{-1} the typical triplet of the GSO structures while the B-type oxyorthosilicates present a doublet degenerated band characteristic of LSO structures [**16, 17, 25**]. So, the LGSO-1 presents the triplet with the main peak at 888 cm^{-1} (denoted in Fig. 5 by a blue square). The doublet associated to ν_3 antisymmetric stretching vibration of $[SiO_4]^{4-}$ tetrahedron is also present at 947 and 1019 cm^{-1}. In opposite, both LGSO-3 as LGSO-5 present two overlapped bands at 887-897 cm^{-1} (green square) and 890-903 cm^{-1} (orange square), respectively, which let us to consider them with LSO structure (Fig. 3, bottom, red spectrum) [8, **25**]. To our knowledge, only Glowacki et al. [10] and Bynczyk et al. [8] reported Raman spectra for LGSO materials with GSO and LSO type structure, respectively. In the first case, the LGSO-1 composition is **close** to $(Lu_{0.13}Gd_{0.865}Sm_{0.005})_2SiO_5$, even considering that due to their small amount and size, the presence of Sm ions does not produce significant changes on the Raman spectrum [10]. So, Table IV summarizes the most significant recorded peaks, identified by software treatment of the data measured for LGSO fibres grown by LFZ. In the case of the LGSO-1 fibres, the Raman spectrum is compared to that obtained by Glowacki et al. [10] for their closer compositions, as mentioned above.

Focusing on the ($\nu_{ext}+\nu_2$) region, which includes modes associated to rare earth ions (T(RE)), translatory and libratory modes associated to SiO_4 anions (T, L(SiO_4)), RE-O stretching vibrations (ν(RE)), and bending vibrations of isolated SiO_4 tetrahedrons ($\nu_2(SiO_4)$) [10], there are two clear differences. The band placed at 348 cm^{-1} for LGSO-1 (blue circle) and at 349 cm^{-1} LGSO-3 (green circle) samples, was also reported for GSO by Voron'ko et al. [**25**] at 344 cm^{-1} with A_g symmetry. Indeed, its intensity is much lower in the LGSO-5 fibres. Furthermore, the main characteristic band **is placed at 403 cm^{-1} for LGSO-5 (orange triangle), at 401 cm^{-1} for LGSO-3 (green triangle) and at 408 cm^{-1} for LSO** [**17**]. In fact, Zheng et al. [**26**] assigned this band, formed by 405 and 411 cm^{-1} peaks, with the ν_2 bending mode. **Likewise**, Voron'ko et al [**25**] reported them at 407 and 413 cm^{-1} with B_g and A_g symmetry, respectively. Thus, these bands, denoted by ν_2(RE-O) [10], are due to vibration modes associated to Gd and Lu **ions**, explaining their variation between materials even when the structure is similar.

Table IV. Raman peaks identified on LGSO fibres by software treatment. LGSO-1 peaks are compared to those identified by Glowacki et al. [10] for $(Lu_{0.15}Gd_{0.845}Sm_{0.005})_2SiO_5$ (noted by 15Lu85Gd) with the corresponding

assignment of vibrations type. Notations from Voron'ko et al. [**25**] are also indicated. Wavenumber values are in cm^{-1}.

LGSO-1	15Lu85Gd [10]		Assignment [10]	LGSO-3	LGSO-5	Region [**25**]
	A_g	B_g				
75	-	-		80	83	
103	-	-		101	98	
117		115				
		132		123	125	
146	144			150	142	
				155	155	
176	175			171		
186		179		182	179	
205		209		195		
213	217		T (RE)	214	195	
223	222		T, L (SiO_4)		214	
230	235		ν(RE-O)	235	235	
239			$\nu_2(SiO_4)$		259	$\nu_{ext}+\nu_2$
280		279		264	285	
301		299		307	293	
315	314			322	315	
					330	
348	347			349	351	
367		366		365	370	
388	384					
	394			401	403	
424	424				427	
443		450				
458	457					
	491					
500		500		516	513	
535		531	$\nu_4(SiO_4)$	529	524	
550	548			550		ν_4
565	555			555	560	
583		581		572	573	
					600	
857	856					
861		865				
888	886			887	890	$\nu_1+\nu_3$
				897	903	
928		926				
947	947		$\nu_1, \nu_3(SiO_4)$	930	935	
				950	945	
1019	1018			962	957	ν_3
				985	962	
		1026		997	970	

The bands placed below 300 cm^{-1} are due to lattice vibrations of cation motion, modes of rare earth species and bending vibrations of the SiO_4 tetrahedra, complicating their assignment [10]. Anyway, two bands can be ascribed based on bibliography. One is the band placed at 264 and 259 cm^{-1}, in LGSO-3 and LGSO-5 fibres, respectively, which was assigned by Zheng et al. [**26**] to ν_2 bending modes of SiO_4 in LSO. On the other hand, a band associated to ν_4 bending modes [**26**] is present around 180 cm^{-1} in all cases, being more intense on LGSO-5 (179 cm^{-1}). Additionally, no vibrational bands of SiO_2 phases [**27**] were identified in any sample.

Finally, the optical behavior of the samples in the UV-visible range was evaluated and quantified by transmission spectroscopy (Fig. 6). This study gave us a first approach about their potential uses in photonic applications. The maximum transmittance measured, with values from 50% up to 77% for the visible range (Fig. 6a), corresponds to LGSO-3 sample as expected from the naked eye inspection (Fig. 1). In contrast, both LGSO-1 as LGSO-5 fibres present lower transmittance due to a scattering effect probably linked to the presence of internal microcracks. Furthermore, the birefringent character of the LSO [**28, 29**] influences these **measurements**. However, the birefringence of biaxial materials as LGSO or LSO, is considered not significant with respect to light output properties of the crystal when, for example, are employed as scintillators [**30**]. Concerning the LGSO-3 fibres, this composition, compared to un-doped oxyorthosilicates, seems to be optimal to reduce stress significantly increasing transparency and should provide good host materials. It must be noted that fringes due to interference phenomena provoked noise signal that are clearly observed on LGSO-3 and LGSO-5 spectra (Fig. 6a). Table V compared transmission values at selected wavelengths for each fibre.

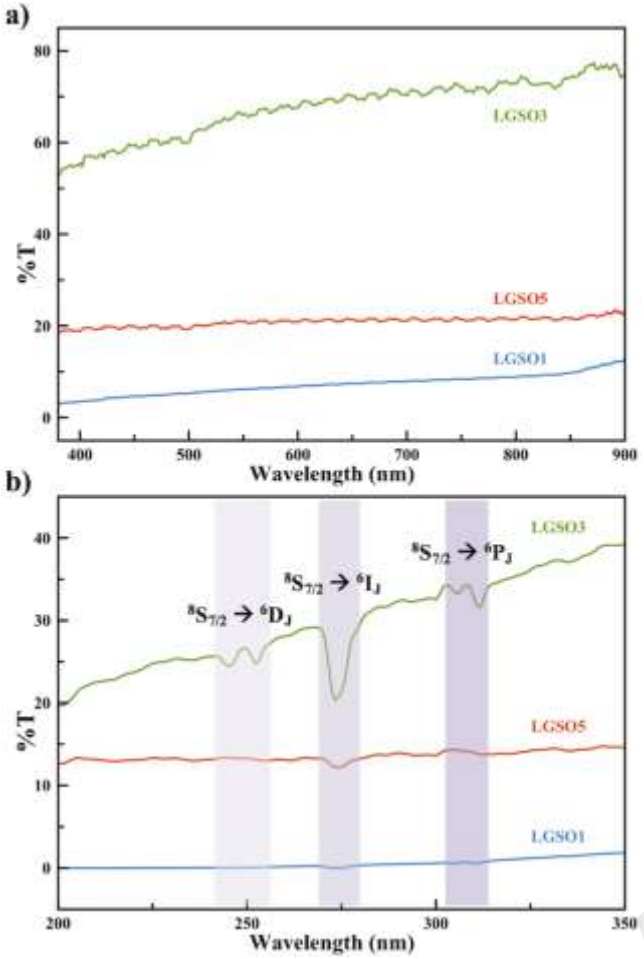

Fig. 6. Transmission spectra of LGSO-1 (blue line), LGSO-3 (green line) and LGSO-5 (orange line) at (a) visible (380-900 nm) and, (b) UV (200-350 nm) regions. Violet areas enclose the bands associated to intra $4f^7$ transitions of Gd^{3+} ions from the $^8S_{7/2}$ ground state [**16**].

Table V. LGSO fibres transmission values at selected wavelengths.

%T	Wavelength (nm)							
Sample	200	275	400	500	600	700	800	900
LGSO-1	0.01	0.05	3.45	5.27	6.77	7.88	8.84	12.55
LGSO-3	19.6	21.36	55.27	60.29	67.56	70.27	72.83	75.23
LGSO-5	12.62	12.29	18.92	19.23	20.79	21.05	21.31	22.95

Focusing on UV range (200-350 nm) and **considering** the doping with optically active elements, a simple approach to photonic behavior was carried out centering our study on the areas corresponding to intra $4df^7$ transitions of Gd^{3+} ions from the $^8S_{7/2}$ ground state (Fig. 7b) [5, **16, 31, 32**]. The main transfer band of the Gd^{3+} ions, that corresponds to $^8S_{7/2} \rightarrow {}^6I_J$ transition, is present in all samples at 275 nm [5, **16, 32**]. However, its intensity is maximum for the LGSO-3 fibres while it is practically absent for LGSO-1. Furthermore, its intensity is higher than un-doped GSO developed by LFZ [**16**]. So, the LGSO-3 fibres should be presumably more efficient laser host materials than un-doped ones due to the energy transfer from Gd^{3+} ions to laser active dopant ions is higher. On the other hand, bands ascribed to $^8S_{7/2} \rightarrow {}^6D_J$ (245 and 252 nm) and $^8S_{7/2} \rightarrow {}^6P_J$ (306 and 311 nm) transitions [5, **16**] were also identified at LGSO-3 spectrum. These correspond to those observed for GSO produced by LFZ [**16**]. Summarizing, the LGSO-3 fibres are good candidates to be doped with optically active ions and these should be optimal to be employed as host materials in photonic applications in agreement with the revised bibliography [10, **24**].

CONCLUSIONS

$(Lu_xGd_{1-x})_2SiO_5$ (LGSO; x=0.1, 0.3 and 0.5) crystalline fibres have been grown in air by the Laser Floating Zone (LFZ) technique at pulling rates of 10 mm/h. The obtained fibres are homogeneous and the presence of macrostructural defects like cracks seems to be lower than observed in GSO fibres also obtained by LFZ. So, as expected, the effect of the Lu^{3+} substitution clearly reduces stress increasing plasticity. Additionally, it was observed that even with a Lu amount up to 0.5 mol.%, no formation of secondary phases like Lu_2O_3 has been detected, in opposite to LSO fibres previously grown by LFZ.

The phase transition, namely from $P2_1/c$ to C2/c, follows the rule stablished within the compositions tested. Indeed, the monoclinic $P2_1/c$ (GSO-type) structure was obtained on LGSO-1 while materials with higher Lu content (LGSO-3 and LGSO-5) presented the C2/c structure (LSO-type). Concomitantly, the Raman spectra have also shown the structural transition from A-type (GSO type) oxyorthosilicates (LGSO-1) to B-type (LSO type) oxyorthosilicates (LGSO-5).

Finally, in the studied spectral range, the transmission studies of LGSO as-grown samples allow to conclude that the trivalent gadolinium ions are optically active presenting an intra-ionic absorption

due to the energy transfer band ascribed to $^8S_{7/2} \rightarrow {}^6I_J$ transition. This band is highest for LGSO-3 samples, which are the most transparent and present lower cracks. Thus, these facts let us to consider the LGSO-3 fibres **as host material** for future uses on photonic applications, i.e. as laser host materials.

ACKNOWLEDGMENTS

This work is funded by FEDER funds through the COMPETE 2020 Programme and National Funds through FCT - Portuguese Foundation for Science and Technology under the project UID/CTM/50025/2013. F. Rey-García acknowledges the Portuguese Science and Technology Foundation (FCT) for the SFRH/BPD/108581/2015 grant.

REFERENCES

[1] R. Lisiecki, G. Dominiak-Dzik, P. Solarz, W. Ryba-Romanowski, M. Berkowski, M. Glowacki, Optical spectra and luminescence dynamics of the Dy-doped Gd_2SiO_5 single crystal, Appl. Phys. B 98 (2010) 337-346.

[2] X. Zhang, Y. Chen, L. Zhou, Q. Pang, M. Gong, Synthesis of a broad-band excited and multicolor tunable phosphor $Gd_2SiO_5:Ce^{3+}$, Tb^{3+}, Eu^{3+} for near-ultraviolet light-emitting diodes, Ind. Eng. Chem. Res. 53 (2014) 6694-6698.

[3] X. Xu, J. Di, J. Zhang, D. Tang, J. Xu, Cw and passively Q-switched laser performance of $Nd:Lu_2SiO_5$ crystal, Opt. Mat. 51 (2016) 241-244.

[4] X. Zhang, J. Xie, X. Chen, L. Fan, D. Lin, Y. Wang, Y. Shi, Fabrication and luminescence properties of polycrystalline Pr^{3+}-doped Lu_2SiO_5 thin films by sol-gel method, J. Alloys Comp. 656 (2016) 735-739.

[5] W. Ryba-Romanovski, A. Strezp, R. Lisiecki, M. Berkowski, H. Rodriguez-Rodriguez, I.R. Martin, Effect of substitution of lutetium by gadolinium on emission characteristics of $(Lu_xGd_{1-x})_2SiO_5:Sm^{3+}$ single crystals, Optical Materials Express 4, 4 (2014) 739-752.

[6] W. Ryba-Romanowski, B. Macalik, M. Berkowski, Down- and up-conversion of femtosecond light pulse excitation into visible luminescence in cerium-doped Lu_2SiO_5-Gd_2SiO_5 solid solution crystals co-doped with Sm^{3+} or Dy^{3+}, Opt. Express 23 (2015) 4552-4562.

[7] V. Bondar, L. Grigorjeva, T. Kärner, O. Sidletskiy, K. Smits, S. Zazubovich, A. Zolotarjovs, Thermally stimulated luminescence on undoped and Ce^{3+}-doped Gd_2SiO_5 and $(Lu,Gd)_2SiO_5$ single crystals, J. Lum. 159 (2015) 229-237.

[8] M. Binczyk, M. Glowacki, A. Lapinski, M. Berkowski, T. Runka, μ-Raman and infrared reflectance spectroscopy characterization of $(Lu_{1-x}Gd_x)_2SiO_5$ solid solution single crystals doped with Dy^{3+} or Sm^{3+}, J. Molec. Struc. 1109 (2016) 50-57.

[9] G. Dominiak-Dzik, W. Ryba-Romanowski, R. Lisiecki, P. Solarz, B. Macalik, M. Berkowski, M. Glowacki, V. Domukhovski, The Czochralski growth of $(Lu_{1-x}Gd_x)_2SiO_5$:Dy single crystals: structural, optical and dielectric characterization, Cryst. Growth Des. 10 (2010) 3522–3530.

[10] M. Glowacki, G. Dominiak-Dzik, W. Ryba-Romanowski, R. Lisiecki, A. Strzęp, T. Runka, M. Drozdowski, V. Domukhovski, R. Diduszko, M. Berkowski, Growth conditions, structure, Raman characterisation and optical properties of Sm-doped $(Lu_xGd_{1-x})_2SiO_5$ single crystals grown by the Czochralski method, J. Solid State Chem. 186 (2012) 268-277.

[11] A. Strzęp, W. Ryba-Romanowski, M. Berkowski, Effect of temperature and excitation wavelength on luminescent characteristics of Lu_2SiO_5–Gd_2SiO_5 solid solution crystals co-doped with Ce^{3+} and Sm^{3+}, Opt. Mater. 37 (2014) 862-865.

[12] G.B. Loutts, A.I. Zagumennyi, S.V. Lavrishchev, Y.D. Zavartsev, P.A. Studenikin, Czochralski growth and characterization of $(Lu_{1-x}Gd_x)_2SiO_5$ single crystals for scintillators, J. Cryst. Growth 174 (1997) 331-336.

[13] Y. Zorenko, V. Gorbenko, V. Savchyn, T. Voznyak, B. Grinyov, O. Sidletskiy, D. Kurtsev, A. Fedorov, V. Baumer, M. Nikl, J.A. Mares, A. Beitlerova, P. Prusa, M. Kucera, Growth and luminescent properties of Lu_2SiO_5:Ce and $(Lu_{1-x}Gd_x)_2SiO_5$:Ce single crystalline films, J. Cryst. Growth 337 (2011) 72-80.

[14] Y. Zorenko, V. Gorbenko, V. Savchyn, T. Zorenko, B. Grinyov, O. Sidletskiy, A. Fedorov, Growth and luminescent properties of Ce and Ce-Tb doped $(Y,Lu,Gd)_2SiO_5$:Ce single crystalline films, J. Cryst. Growth 401 (2014) 577-583.

[15] G.F. de la Fuente, L.R. Black, D.M. Andrauskas, H.R. Verdún, Growth of Nd-doped rare earth silicates by the laser floating zone method, Solid State Ionics 32/33 (1989) 494-505.

[**16**] F. Rey-García, N. Ben Sedrine, M.R. Soares, A.J.S. Fernandes, A.B. Lopes, N. Ferreira, T. Monteiro, F.M. Costa, Structural and optical characterization of Gd_2SiO_5 crystalline fibres obtained by Laser Floating Zone, Opt. Mater. Express 7, 3 (2017) 868-879.

[**17**] F. Rey-García, N. Ben Sedrine, A.J.S. Fernandes, T. Monteiro, F.M. Costa, **Shifting Lu_2SiO_5 crystal to eutectic structure by laser floating zone", J. Eur. Ceram. Soc. 38, 4 (2018) 2059-2067**.

[**18**] M. R. B. Andreeta and A. C. Hernandes, "Chapter 13: Laser-Heated Pedestal Growth of Oxide Fibers," in Springer Handbook of Crystal Growth, Dr. G. Dhanaraj, Prof. K. Byrappa, Dr. V. Prasad, and Prof. M. Dudley, eds. (Springer Verlag, 2010).

[**19**] P. Rudolph (editor), Handbook of Crystal Growth (2nd edition), Elsevier, 2015.

[20] R.S. Roth, S.J. Schneider, Phase equilibria in systems involving the rare-earth oxides. Part I. Polymorphism of the oxides of the trivalent rare-earth ions, J. Research Natl. Bur. Standards 64, 4 (1960) 309-316.

[21] S.C. Atkinson, "Crystal structures and phase transitions in the rare-earth oxides", Doctoral Thesis, University of Salford (UK), 2013.

[**22**] R. G. Carvalho, A. J. S. Fernandes, F. J. Oliveira, E. Alves, N. Franco, C. Louro, R. F. Silva, F. M. Costa, Single and polycrystalline mullite fibres grown by laser floating zone technique, J. Eur. Ceram. Soc. 30, 16 (2010) 3311–3318.

[**23**] International Centre for Diffraction Data, (2017). http://www.icdd.com (accessed 2017.07.20)

[**24**] O.T. Sidletskiy, V.G. Bondar, B.V. Grynyov, D.A. Kurtsev, V.N. Baumer, K.N. Belikov, Z.V. Shtitelman, S.A. Tkachenko, O.V. Zelenskaya, N.G. Starzhinsky, V.A. Tarasov, Growth of LGSO:Ce crystals by the Czochralski method, Crystall. Reports 54 (2009) 1256-1260.

[**25**] Y.K. Voron'ko, A.A. Sobol, V.E. Shukshin, A.I. Zagumennyi, Y.D. Zavartsev, S.A. Koutovoi, Spontaneous raman spectra of the crystalline, molten and vitreous rare-earth oxyorthosilicates, Opt. Mater. 33, 8 (2011) 1331-1337.

[**26**] L. Zheng, G. Zhao, C. Yao, X. Xu, L. Su, Y. Dong, J. Xu, Raman spectroscopic investigation of pure and ytterbium-doped rare earth silicate crystals, J. Raman Spectrosc. 38 (2007) 1421-1428.

[**27**] V.K. Malinovsky, V.N. Novikov, N.V. Surotsev, A.P. Shebanin, Investigation of amorphous states of SiO_2 by Raman scattering spectroscopy, Physics of the Solid State 42, 1 (2000) 65-71.

[**28**] S. Roy, H. Lingertat, C. Brecher, V.K. Sarin, Spectroscopic and Transmittance properties of fine grained Ce^{3+} doped lutetium oxyorthosilicate, IEEE Trans. Nuc. Sci. 59, 5 (2012) 2587-2593.

[**29**] G.E. Jellison Jr, E.D. Specht, L.A. Boatner, D.J. Singh, C.L. Melcher, Spectroscopic refractive indices of monoclinic single crystal and ceramic lutetium oxyorthosilicate from 200 to 850 nm, J. Appl. Phys. 112 (2012) 063524.

[**30**] G. Erdei, N. Berze, A. Péter, B. Játékos, E. Lórincz, Refractive index measurement of cerium doped $Lu_xY_{2-x}SiO_5$ single crystal, Opt. Mater. 34 (2012) 781-785.

[**31**] G. Blasse, B.C. Grabmaier, Luminescent Materials, Springer, Berlin (1994).

[**32**] A. Lushchik, V. Nagirnyi, E. Shablonin, O. Sidletskiy, B. Toxanbayev, A. Zhunusbekov, Luminescence of cations excitons in Gd_2SiO_5 crystals,
http://photon-science.desy.de/annual_report/files/2009/2009545.pdf (accessed 2017.07.20)

Table I. LFZ experimental conditions **and comparison to pure GSO [16] and LSO [17] also grown in descendent direction on air by LFZ**.

Sample	Nominal formula	Diameter (mm)	Pulling rate (mm/h)	Power (W)	Ref.
GSO	Gd_2SiO_5	1.5	10	72	**16**
LGSO-1	$(Lu_{0.1}Gd_{0.9})_2SiO_5$	1.5	10	67	-
LGSO-3	$(Lu_{0.3}Gd_{0.7})_2SiO_5$	1.5	10	58	-
LGSO-5	$(Lu_{0.5}Gd_{0.5})_2SiO_5$	1.5	10	64	-
LSO	Lu_2SiO_5	2	10	92	**17**

Table II. Initial and calculated compositions determined by EDS analysis.

Sample	Initial composition	EDS calculated composition
LGSO-1	$(Lu_{0.1}Gd_{0.9})_2SiO_5$	$(Lu_{0.12}Gd_{0.88})_2SiO_5$
LGSO-3	$(Lu_{0.3}Gd_{0.7})_2SiO_5$	$(Lu_{0.31}Gd_{0.69})_2SiO_5$
LGSO-5	$(Lu_{0.5}Gd_{0.5})_2SiO_5$	$(Lu_{0.53}Gd_{0.47})_2SiO_5$

Table III. XRD most intense peaks, corresponding planes and intensity for LGSO-3, LGSO-5 and LSO [**17**].

LGSO-3			LGSO-5			LSO [**17**]		
Peak	Plane	Intensity (%)	Peak	Plane	Intensity (%)	Peak	Plane	Intensity
22.7º	($\bar{3}$ 1 1)	99.7	22.9º	($\bar{3}$ 1 1)	89.8	23.2º	($\bar{3}$ 1 1)	92.6
29.3º	($\bar{3}$ 1 3)	85.8	28.5º	(0 2 1)	93.7	29.9º	($\bar{3}$ 1 3)	100
30.5º	(2 0 2)	100	30.8º	(2 0 2)	100	31.2º	(2 0 2)	95.5

Table IV. Raman peaks identified on LGSO fibres by software treatment. LGSO-1 peaks are compared to those identified by Glowacki et al. [10] for $(Lu_{0.15}Gd_{0.845}Sm_{0.005})_2SiO_5$ (noted by 15Lu85Gd) with the corresponding assignment of vibrations type. Notations from Voron'ko et al. [**25**] are also indicated. Wavenumber values are in cm^{-1}.

LGSO-1	15Lu85Gd [10]		Assignment [10]	LGSO-3	LGSO-5	Region [**25**]
	A_g	B_g				
75	-	-		80	83	
103	-	-		101	98	
117		115				
		132		123	125	
146	144			150	142	
				155	155	
176	175			171		
186		179		182	179	
205		209		195		
213	217		T (RE)	214	195	
223	222		T, L (SiO_4)		214	
230	235		ν(RE-O)	235	235	
239			$\nu_2(SiO_4)$		259	$\nu_{ext}+\nu_2$
280		279		264	285	
301		299		307	293	
315	314			322	315	
					330	
348	347			349	351	
367		366		365	370	
388	384					
	394			401	403	
424	424				427	
443		450				
458	457					
	491					
500		500		516	513	
535		531	$\nu_4(SiO_4)$	529	524	
550	548			550		ν_4
565	555			555	560	
583		581		572	573	
					600	
857	856					
861		865				
888	886			887	890	$\nu_1+\nu_3$
				897	903	
928		926	$\nu_1, \nu_3(SiO_4)$			
947	947			930	935	
				950	945	
1019	1018			962	957	ν_3
				985	962	
		1026		997	970	

Table V. LGSO fibres transmission values at selected wavelengths.

%T	Wavelength (nm)							
Sample	200	275	400	500	600	700	800	900
LGSO-1	0.01	0.05	3.45	5.27	6.77	7.88	8.84	12.55
LGSO-3	19.6	21.36	55.27	60.29	67.56	70.27	72.83	75.23
LGSO-5	12.62	12.29	18.92	19.23	20.79	21.05	21.31	22.95